

Prediction of relative permeability in simple porous media

Steven Bryant* and Martin Blunt

BP Research Centre, Chertsey Road, Sunbury-on-Thames, Middlesex TW16 7LN, United Kingdom

(Received 12 December 1991)

We present a predictive calculation of two-phase relative permeabilities in granular porous media formed from a dense random packing of equal spheres. The spatial coordinates of every sphere in the pack have been measured, enabling the microstructure of the medium to be completely determined. From these data we extract a network model that replicates the pore space. By compacting the packing or swelling individual spheres, we may generate model porous media of different porosities whose microstructure is also completely determined. We simulate both viscous- and capillary-dominated invasion of a nonwetting fluid into a wetting fluid contained in these media. During invasion we calculate the average hydraulic conductance of each phase to obtain the relative permeabilities as a function of fluid saturation. Because the microstructure is known, the calculations do not involve any adjustable parameters or supplementary measurements of pore structure. The computed relative permeabilities are successfully compared with experimental values previously measured on sand packs, bead packs, and a simple sandstone.

PACS number(s): 47.55.Mh, 64.60.Ak

I. INTRODUCTION

Relative permeability and capillary pressure are mesoscopic transport properties that describe the simultaneous flow of immiscible fluids in porous media. At the pore scale fluids reside in intergranular spaces whose dimensions in typical sedimentary rocks are on the order of tens of micrometers. The displacement of one fluid by another is controlled by surface tension, viscous forces, and the geometry of the pore space. The relative hydrodynamic conductance of each fluid at a given saturation is the relative permeability, while the pressure difference between the phases is the capillary pressure. These two functions determine the macroscopic fluid flow behavior in hydrocarbon reservoirs over the scale of centimeters to kilometers.

Computer models using an idealized pore structure and displacement mechanisms have been used to model two-phase flow in porous media, starting with the work of Fatt [1]. The void space of the medium is represented as a network of large spaces (pores) connected by thinner restrictions (throats). By judicious choices for the distribution of pore and throat sizes and the coordination number of the network it is possible to compute relative permeabilities that are similar to measured values, although there is no independent assessment of whether the model structure actually replicates the real structure. Salter and Mohanty [2] and Heiba *et al.* [3] matched numerical relative permeabilities and capillary pressure to experiments on carefully prepared core samples. More recently Jerauld and Salter [4] have made predictions for the displacement behavior in a variety of different conditions. While the microscopic flow processes may be determined by considering capillary equilibrium or by viewing fluid motion in two-dimensional etched glass networks (Lenormand and co-workers [5,6], Furuberg *et al.* [7], Diaz, Chatzis, and Dullien [8], Dias and Payatakes [9]), it has

proved much more difficult to construct a reliable three-dimensional representation of a rock from which predictions of transport properties may be made. So far the best attempts have concentrated on predicting single-phase permeability, and include using simple correlations involving a typical pore radius (Katz and Thompson [10], MacGowan [11]) and ambitious projects where an explicit computer model of the pore space was built from successive two-dimensional images of a rock sample (Koplik, Lin, and Vermette [12], Yanuka, Dullien, and Elrick [13]).

A random close packing of monodisperse spheres is a simple yet realistic model of an unconsolidated well-sorted sandstone. Such a packing can be transformed into a model of a consolidated sandstone by allowing the spheres to swell without moving their centers. This is a reasonable approximation of the process of quartz cementation in the Earth's crust. Such cementation coats the grains with more material, fusing them together and lowering the porosity.

Finney measured the coordinates of a random close pack of 8000 ball bearings [14]. This data permits construction of a precise replica of the void space of a real porous medium without the difficulties of serial sectioning. Using the Finney pack as a starting point, Bryant and co-workers [15,16] have predicted single-phase permeability and capillary pressure for simple rocks of different porosities. The predictions are in excellent agreement with measurements on Fontainebleau sandstones and bead and sand packs.

In this paper we will use the Finney pack to predict from first principles the drainage relative permeabilities for monodisperse granular porous media as a function of porosity. This is achieved by having a complete description of the pore space and a careful representation of the two-phase displacement [17]. The predictions closely match experimental data. Two-phase flow properties

have been genuinely predicted without the use of adjustable parameters or additional measurements of pore structure.

Predictions of the amount of oil recovered, or the sensitivity of the recovery to the injection of displacing gas or water, are crucially dependent on the relative and absolute permeability everywhere in the reservoir. Although the rock type and fluid properties are likely to change drastically through the reservoir, the only samples of rock come from drilling wells, which represent a tiny fraction of the total volume in a reservoir. Furthermore, relative permeability measurements on these samples are difficult and time consuming. To quantify and control uncertainty in recovery calculations, it is necessary to have some theoretical understanding of transport properties. Such understanding would enable us to predict the sensitivity of relative permeability and capillary pressure to geological factors such as porosity, rock type, the degree of compaction, and the nature of the fluids. This work is a preliminary step in this direction. Though we present comparisons with particular sandstone samples, such predictions are not the primary objective of this work. (Indeed, given a sandstone sample it is probably more straightforward to measure its relative permeability curves than to predict them using either our approach or previously published models.) A more important result is that we are now able to quantify the change in the relative permeability for similar but underground and unobtainable samples if, for instance, we can estimate the degree of compaction of cementation. Such estimates can be derived from models of the geological history of the reservoir. Also for a statistical geological map of the rock type or absolute permeability, we may supply estimates of the corresponding relative permeabilities.

II. MODEL OF SIMPLE GRANULAR POROUS MEDIA

One way to predict transport properties in porous media is to use an exact representation of the pore space. A random close packing of equal spheres is a simple but reasonable idealization of an unconsolidated sediment of well-sorted quartz grains. Finney [14] constructed an isotropic random sphere pack from 17 000 precision ball bearings and then painstakingly measured the positions of approximately 8000 spheres in the center of the pack. From this data we can construct a complete description of the pore space.

A. Division into Delaunay cells

A Voronoi tessellation of a set of points in three dimensions divides a space into polyhedra that enclose the volume nearer to a given point than any other. The Delaunay dual of this network divides the space into tetrahedra [18]. The edges of each tetrahedron connect four nearest-neighbor points.

A Delaunay construction has been performed on the central 3367 spheres of the Finney pack [19]. The points are the sphere centers. The vertices of the Delaunay cells lie at the sphere centers, while the interior of the cell

closes a region of void space as shown in Fig. 1. Each cell face is a plane of maximum constriction or maximum curvature of the pore space and thus represents a narrow entrance to the wider void inside the cell.

We wish to construct an equivalent network model of the pore space. The network model consists of pores or void spaces connected by narrower constrictions or throats. We may identify the pores with the interior of the Delaunay cells and the throats with the faces—each cell represents a pore and each cell face is a throat. For calculating relative and absolute permeabilities we assume that all the viscous pressure drops occur across the throats.

From the Delaunay tessellation of the central 3367 spheres we find approximately 15 000 pores and 30 000 throats. Since each cell is a tetrahedron, every pore has four throats leading from it—the coordination number of the network is 4.

B. Geometry of the network

To calculate absolute and relative permeabilities as a function of saturation we must assign equivalent radii and hydraulic conductivities to the throats and volumes to the pores. The pore volume is the Delaunay cell volume minus the volumes of the segments of spheres contained within it. The aggregation of cell pore volumes is used to calculate the porosity of the network and the fluid saturation when different cells are occupied by different fluids.

The flow paths between adjacent cells are modeled by cylinders whose radii and length are hydrodynamically equivalent to the real pore space. The absolute permeability is then the fluid conductivity of the network of cylinders. The flow resistance of the junctions of the cylinders is ignored. For steady incompressible flow in a conduit we expect a relation of the form

$$Q = g \Delta P , \quad (1)$$

where Q is the volume of fluid entering or leaving the medium in unit time, ΔP is the pressure drop, and g is defined as the hydrodynamic conductivity. For Poiseuille flow in a cylinder of radius r and length l ,

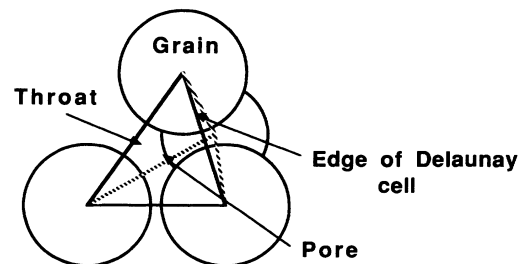


FIG. 1. Delaunay cell in a random close packing of spheres. In the center of the tetrahedral cell is a void space or pore and crossing each face are four narrower restrictions called throats. The vertices of the cells are situated at the sphere centers.

$$g = \frac{\pi r^4}{8\mu l}, \quad (2)$$

where μ is the fluid viscosity. For each flow path (throat) in our network, we need to find values of r and l that give the correct conductivity g in Eq. (1).

The throat may be represented by a cylinder of radius r_{eff} , which has the same conductivity as the flow path between adjacent cells. We could solve the Navier-Stokes equation by a finite element technique in the void space to find this effective radius. In Ref. [15] an approximate numerical solution was used to find r_{eff} in a typical conduit. The conductivity of the flow path was found to be dominated by the narrowest constriction along the path, which occurs at the face shared by the cells. As illustrated in Fig. 2, the effective cylinder radius may thus be estimated by r_c , the largest circle that can be inscribed in this cross section. Another estimate is r_e , the radius of the circle having the same area as the cross section. r_c underestimates the conductivity, while r_e is an overestimate, since for fixed area a circle is the most efficient cross section for fluid flow. It was found that the average of r_c and r_e , $r_{\text{eff}} = \frac{1}{2}(r_c + r_e)$, gave a good estimate of the effective radius [15]. This approximation for r_{eff} was motivated by a study of the geometry of the pore space—it is not adjusted to fit the experimental measurements of permeability.

The effective flow path length is defined to be the distance between the centers of the adjoining cells. The center of a cell is taken to be the point equidistant from the centers of the four spheres that define the cell. In some cases the cell center may lie outside the volume enclosed by the cell faces (the pore). For convenience in defining path lengths, such cell centers are projected onto the nearest cell face.

The slow invasion of a nonwetting fluid into a porous medium is controlled by capillary forces. As we describe in more detail in the next section, the invading fluid is first able to enter and fill a pore when the injection pressure is sufficient to overcome the capillary pressure neces-

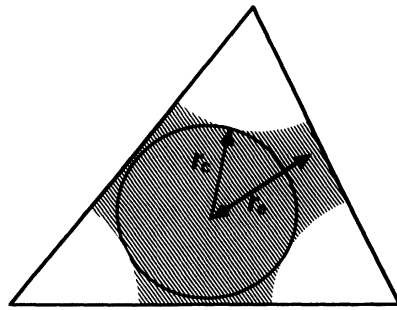


FIG. 2. Two definitions of an equivalent throat radius. One face of a Delaunay cell is shown. r_c has the radius of the largest circle that can fit in the cross section of the void space with the cell edge. r_e is the radius of the circle whose area is equal to the void area (shaded). A good estimate of the true hydrodynamic radius is $r_{\text{eff}} = \frac{1}{2}(r_c + r_e)$.

sary to pass through a throat. This pressure is inversely proportional to an equivalent capillary radius of the throat. A good approximation of this radius, due originally to Haines, is the insphere radius of the cell face r_c [20].

Thus the network is specified by (i) its topology, that is, which pores are connected by which throats, (ii) the equivalent conductivities $g = \pi r_{\text{eff}}^4 / 8\mu l$ and insphere radii r_c of the throats, and (iii) the volumes of the pores. All this information is derived directly from Finney's original measurements of sphere center coordinates in the packing. None of it is adjusted to fit the experimental data.

C. Modeling compaction and cementation

We have shown how to construct the equivalent network model for an unconsolidated random sphere pack. We can also construct model rocks of varying porosity by simulating the effect of processes such as compaction during burial and cementation [16].

We model a compacted sandstone by moving the centers of the spheres closer together in one (the vertical) direction. We rescale one of Finney's coordinate axes by

$$z' = z_0 + \lambda(z - z_0), \quad (3)$$

where z_0 is an arbitrary reference value and λ measures the degree of compaction. The spheres then interpenetrate. We assume that in the compaction process the material corresponding to the intersecting grains has dissolved under pressure. This pressure-dissolved material can be washed out of the system or reprecipitated, depending upon prevailing physical conditions.

At depth within the earth's crust, quartz cement often precipitates on the sand grains of compacted rock to form approximately concentric overgrowths. We model this by increasing the radius of the spheres uniformly without altering the position of the sphere centers. Thus the grains will appear to have interpenetrated, though in fact a layer of uniform thickness has been deposited only upon their exposed surfaces.

The Delaunay tessellation is unchanged for the model of quartz overgrowth, but a new arrangement of cells needs to be constructed for the compacted rocks (because compaction moves the sphere centers relative to one another). The equivalent hydrodynamic network is constructed as before. At porosities lower than about 10% some of the cell faces become completely blocked; their conductivity and effective radius are zero. The unconsolidated material has a porosity of 36.2%. At a porosity of approximately 3% for both compacted and overgrowth-cemented rock the overall conductivity of the rock falls to zero. At this point about half the cell faces are closed and there are no open pathways through the whole pack [16,21].

III. SINGLE-PHASE FLOW

The calculation of absolute permeability and the comparison with measured values is described in greater detail elsewhere [15,16], but is repeated briefly here for completeness.

A. Computing absolute permeability

The equivalent network model tells us how to compute the flow in each cylinder. For the k th cylinder $Q_k = g_k \Delta P_{ij}$, where ΔP_{ij} is the pressure difference between the centers of the pores labeled i and j , which are connected via throat k . Mass conservation at each pore requires

$$\sum_k Q_k^i = 0, \quad (4)$$

where the sum runs over the throats k ($k = 1$ to 4) connected to pore i . Equation (4) is solved by Gauss-Seidel iteration with overrelaxation.

The portion of the Finney pack from which we have constructed our network is roughly spherical. It is thus convenient to impose an approximately spherically symmetric pressure gradient by fixing the pressure in a spherical region at the center of the pack (the inlet) and at the external boundary (the outlet). If we define the outlet pressure to be zero and the inlet pressure to be unity, then the permeability of the network K is defined by

$$K = \frac{Q_{\text{tot}} \mu}{4\pi} \left(\frac{1}{r_{\text{in}}} - \frac{1}{r_{\text{out}}} \right). \quad (5)$$

Q_{tot} is the total flow, r_{in} is the radius of the inlet, and r_{out} is the radius of the outlet boundary.

B. Comparisons with measured values

Permeability has the units of length squared. The calculated permeability of the unconsolidated pack is $2.8 \times 10^{-4} d^2$, where d is the sphere diameter. Refinements to the calculation of r_{eff} and l give a value of $6.8 \times 10^{-4} d^2$, which compares well with data collected from random sphere packs composed of beads of different materials and sizes [15]. The refined definitions of r_{eff} and l better represent the real flow paths, but their calculation is geometrically somewhat involved. Trials showed that the refinements do not significantly affect the computed *relative* permeabilities, so for simplicity we will use the above definitions of r_{eff} and l for the simulation of two-phase flow.

A series of computations described in another paper [16] showed that in well-sorted rocks (i.e., rocks with narrow grain size distributions) both compaction and overgrowth cementation have virtually the same effect on permeability as a function of porosity. Figure 3 shows the predicted permeability using the overgrowth model compared with a series of 240 measurements on Fontainebleau sandstone performed by Bourbie and Zinszner [22]. The Fontainebleau sandstone is composed of well-sorted fine sand grains of pure quartz. The only difference between samples is the degree of quartz cementation. Because permeability is a dimensional quantity, a length scale must be introduced to compare the predictions with measurements. This is taken from an estimate of the mean grain size before cementation, which is inferred from Sieve analysis and the examination of thin sections. Cathodoluminescence enabled Bryant, King, and Mellor

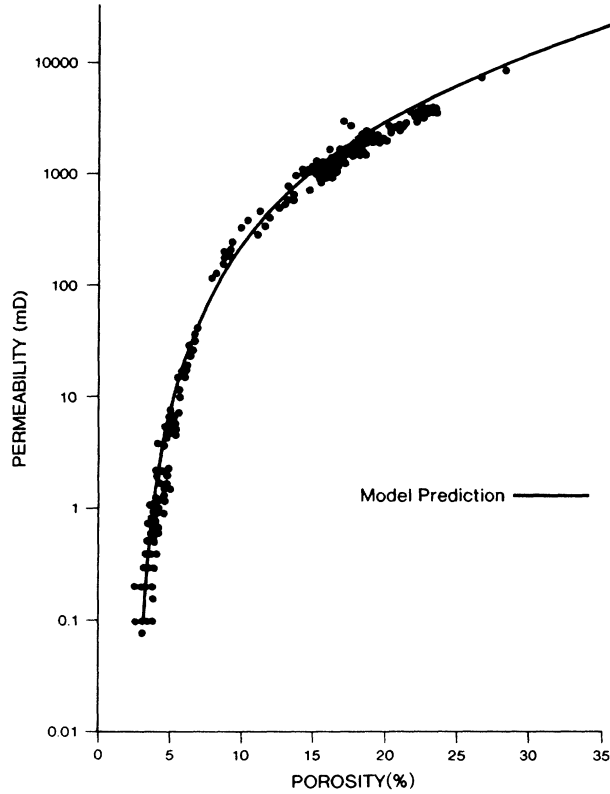


FIG. 3. Comparison of predicted absolute permeability [in millidarcy (mD) units] as a function of porosity for monodisperse consolidated granular rocks with measurements on Fontainebleau sandstone [22].

[15] to distinguish the overgrowth from the original grains. They found an average grain diameter of approximately 0.4 mm.

In Fig. 3 the trend of permeability with porosity, spanning five orders of magnitude is excellently predicted. This demonstrates that the model of cementation of a random sphere pack and its network representation of the pore space are adequate to predict the average behavior in single-phase flow, which implies that the location and conductivities of the major flow paths have been accurately identified.

IV. TWO-PHASE FLOW

We wish to simulate two-phase flow in our model porous media. We inject a nonwetting fluid into a material that is originally full of wetting fluid. At low flow rates the fluid motion is controlled by capillary forces. The description of the flow process follows (Ref. [17]).

A. Capillary equilibrium

Consider two immiscible fluids at rest in a porous medium. If one phase is completely wetting, a thin film will coat all the solid surfaces and will coat any small ($< 1 \mu\text{m}$) irregularities on the grains. There will also be curved surfaces between the two fluids with a pressure drop ΔP across the interface because of the surface tension

$$\Delta P = \gamma \left(\frac{1}{r_1} + \frac{1}{r_2} \right), \quad (6)$$

where γ is the surface tension and r_1 and r_2 are the principal radii of curvature of the interface. For a cylindrical throat of radius r ,

$$\Delta P = -\frac{2\gamma \cos\theta}{r}, \quad (7)$$

θ is called the contact angle and is the angle at which the fluid interface approaches the solid surface. If $\theta > 90^\circ$ there is a decrease in pressure across the boundary—the pressure is higher in the nonwetting fluid.

ΔP is very large for any interface in or across tiny crevices in the porous medium, since a radius of curvature will be small. Thus, if there are small channels or corrugations along the pore-grain surface, the wetting phase will preferentially fill them. The wetting phase is thus likely to be hydraulically connected throughout the rock along a network of sub-pore-scale roughness.

Imagine now the rate-controlled injection of a nonwetting fluid. The injection pressure is increased slowly. Normally the fluid interfaces in the medium will move only a short distance before coming to rest in equilibrium in slightly narrower regions of the pore space than before. Eventually one interface will reach the narrowest part of a throat before entering a wider pore space. Having filled the pore, the fluid interface becomes constrained by the narrow channels leading from this pore, and the injection pressure rises. The next pore to be filled will be connected to an already filled pore via a restriction with the lowest entry pressure.

At every stage in the displacement the nonwetting fluid advances through the throat with the lowest entry pressure. For our model porous media, this entry pressure is controlled by the insphere radius r_c of the throat. We assume that the injected fluid is strongly nonwetting and take $\theta = 180^\circ$. Thus

$$P_{\text{entry}} = -\frac{2\gamma}{r_c}. \quad (8)$$

The lowest entry pressure corresponds to the largest radius r_c .

B. Simulating drainage

Initially the network is full of wetting fluid. Nonwetting fluid is allowed access to the network through a fraction of the faces or throats chosen at random on the outer boundary of the pack. Following Ref. [19], this fraction was chosen to be about 1% in order to minimize finite-size effects. The restricted access applies only to the simulation of drainage; for calculation of relative permeabilities no such restrictions are necessary.

The throats and pores are filled one at a time. A throat is considered available if it contains no injected fluid, but is connected to a pore that does. At each stage the available throat with the largest insphere radius r_c is filled, together with any empty (filled with wetting fluid) pore attached to it. This is the invasion percolation model of

drainage first proposed by Chandler *et al.* [23] and Wilkinson and Willemsen [24].

We assume that the wetting fluid is everywhere hydraulically connected. This means that we ignore trapping of the displaced phase—the nonwetting fluid can always enter a throat or pore and the wetting fluid can always escape along a microscopic wetting film. This is also equivalent to an infinitely compressible displaced phase.

This model has been used to simulate mercury injection [20]. Mercury is nonwetting and is injected into an evacuated rock sample. The entry pressure, Eq. (8) as a function of the saturation of injected fluid, is called the capillary pressure. The predicted capillary pressure curves for rocks of different porosity have been successfully compared with experimental measurements on Fontainebleau sandstone [16]. This paper will concentrate solely on the prediction of relative permeability.

C. Calculating relative permeability

In its most general form a linear relationship between flow rate Q and pressure gradient may be written as [25–32]

$$Q_1 = -\lambda_{11}\nabla P_1 - \lambda_{12}\nabla P_2, \quad (9)$$

$$Q_2 = -\lambda_{22}\nabla P_2 - \lambda_{21}\nabla P_1. \quad (10)$$

The mobility tensor λ_{ij} may be written as Kk'_{ij}/μ_i , where k'_{ij} are called the relative permeabilities, which are some fraction of the absolute permeability K . The phase pressures P_1 and P_2 differ by the capillary pressure [33]

$$P_{\text{cap}}(S) = P_2 - P_1, \quad (11)$$

where the labels 1 and 2 refer to the wetting and nonwetting fluids, respectively.

In two-phase immiscible flow, the two fluids reside in different subsections of the pore space. For flow at an infinitesimal rate, with no displacement, the fluids move through these separate subsections with no interaction between the phases. In this case the off-diagonal terms λ_{12} and λ_{21} are zero and there is simply a hydraulic conductance associated with each phase, which is some fraction of the single-phase value K . This fraction is called the relative permeability k' . k' depends purely on the fluid configuration at a given saturation. For a given type of displacement k' may be written as a function of one of the phase saturations only (normally the wetting phase saturation S) [25,26]. In general, as demonstrated by many authors theoretically and experimentally [27–32], this assumption is incorrect and there is a viscous coupling between the two phases, which leads to non-negligible off-diagonal terms in the mobility tensor. Viscous coupling is certainly significant in the mobilization of trapped oil ganglia and for high rate countercurrent flows [31], and an assessment of its importance in other situations is a subject of active research. In this paper we model quasistatic floods, where the off-diagonal terms in λ_{ij} are zero, or (as described later) very high rate flow where $P_1 = P_2$ and these terms are ill-defined. The

experiments we compare against did not consider them, and assumed implicitly (in common with most of the literature) that they were zero. Inclusion of viscous coupling by postulating off-diagonal terms qualitatively similar to those measured experimentally [31] would have made our predictions worse in all cases. We consider that in the systems we analyze here—well-connected sandstones with no trapping in primary drainage—viscous coupling may be neglected.

To compute the relative permeabilities we need to define the saturation and hydraulic conductance. When the nonwetting fluid passes through a throat it is assumed to fill completely the pore connected to it except for pendular rings of the wetting phase clinging to the narrow crevice between two spheres, see Fig. 4. We define a capillary pressure drop by P_{entry} , Eq. (8), where r_c is the last throat invaded. We then calculate the position of pendular rings consistent with this capillary pressure, using Eq. (6). The two radii of curvature r_1 and r_2 are the radius from the axis joining the two grains that contain the ring and the radius of curvature of the interface connecting the two spheres, with a contact angle of 180° . The volume of these rings is used in the calculation of saturation. These rings do not intersect and so they do not contribute to the conductivity of the wetting phase. The volume of the nonwetting phase also includes the bulges protruding from each uninvaded face from a pore filled with invading fluid. The radius of curvature of the surface (assumed to be a segment of a sphere) is found from the capillary pressure.

The computation of the permeability of each phase is identical to the calculation for single-phase flow except that each phase is considered to occupy a separate subnetwork of the pore space. The effective throat radii and lengths are the same. A throat is considered to be open for flow of the nonwetting phase if it has been invaded. Also, adjacent cells containing nonwetting phase are checked for faces that have not been invaded according to the hemisphere criterion Eq. 8, but would have had surfaces protruding from each cell through the plane of the face. Such faces were counted open for nonwetting phase flow under the assumption that a saddle surface of lower curvature (and therefore lower free energy) would have spontaneously formed. A throat is open for flow of the wetting phase only if it is closed for the nonwetting

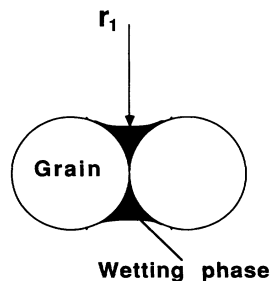


FIG. 4. The wetting fluid clings to the grain surfaces in pendular rings. The two principal radii of curvature of the rings are r_1 , as shown, and r_2 , the radius of curvature out of the plane of the diagram.

phase and connects two pores, neither of which have been invaded. Although the wetting phase is assumed to be hydraulically connected everywhere along microscale surface roughness, the contribution to the permeability of this flow is negligible—the crevice radii are typically $1 \mu\text{m}$, against 10 to $100 \mu\text{m}$ for the throats, and the conductivity is proportional to the channel radius raised to the fourth power. Special consideration is required for throats that form the exterior boundary of the network, since these do not terminate in an explicit pore. To determine phase conductivities for a boundary throat, we create a virtual neighboring pore containing the same phase as the network pore. We then apply the rules given above for interior throats.

The relative permeabilities are computed at about ten stages during a displacement. The computation is only performed if the entry pressure has reached a previously unattained maximum—thus the simulation records the fluid configuration and conductivities as a function of strictly increasing capillary pressure. At extreme saturations the subnetwork of the minor phase does not extend to the center of the packing. Hence for relative permeability calculations it is convenient to assign a uniform pressure to a central core of the network (typically of radius 2 to 3 sphere diameters) rather than to the central cell as in single-phase computations. Because the flow field is spherical, inhomogeneities in the saturation distribution have a disproportionate effect on calculated relative permeabilities. As a result, the global saturation is rarely a good indicator of the local phase fraction that dominates the relative permeabilities. To obtain representative values of saturation at each stage of displacement, we average the local saturations over ten concentric shells of equal thickness.

Performing the simulation in a cuboidal section of the Finney pack, $19 \times 19 \times 7$ sphere diameters in extent produced almost identical results. The inlet and outlet were the 19×19 faces of the cuboid. This linear flow geometry is relatively insensitive to saturation inhomogeneities, and the result supports the representativeness of the radial average saturation described above.

D. Comparison with experiment

Figure 5 shows measured and predicted relative permeability curves in two unconsolidated well-sorted systems. The data for the first system, obtained at a low flow rate in a bead pack [34], are typical of similar experiments reported by other investigators [35]. The predicted relative permeabilities were computed as described above for the original Finney pack (no compaction or cementation). The predicted nonwetting phase curve is in good agreement with the experimental data. The wetting phase relative permeability is not such a good match. It appears that the permeability is overestimated or the wetting phase saturation is underestimated. The latter is more likely. While the wetting phase clinging to small crevices in the pore-grain surface may make a tiny contribution to the relative permeability, it may add a few percent to the saturation. Our calculations ignore this correction, and without some independent knowledge of

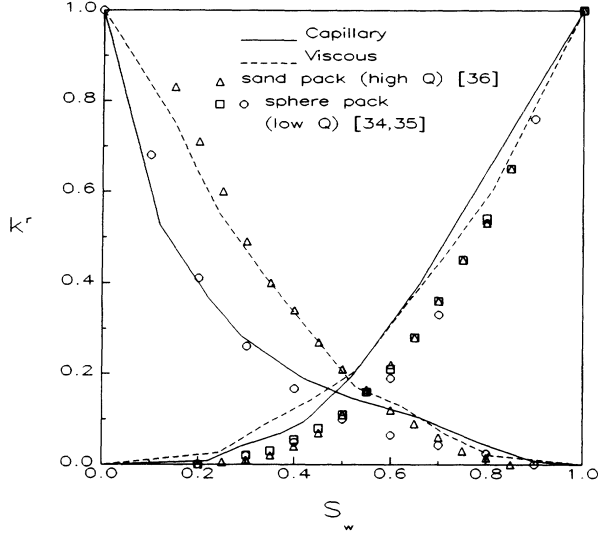


FIG. 5. Predicted and experimental measurements of drainage relative permeability in unconsolidated porous media. The triangles are high flow rate measurements [36], while the circles and squares are values measured at low flow rates [34,35]. The predicted curves are computed assuming capillary controlled displacement (solid line) or a viscous-dominated flood (dashed line).

the exact structure of the grain surfaces it is impossible to estimate its importance reliably.

The second set of curves comes from an experiment on a sand pack performed at a high rate [36], considerably greater than normally seen in reservoir displacements. For the fluid configuration to be controlled by capillary forces, the capillary number C_A , which is the ratio of typical viscous to capillary pressure drops across a throat containing a fluid interface, must be much less than 1. If we define

$$C_A = \frac{4l\mu Q}{\gamma r_c}, \quad (12)$$

where Q is the volumetric flow rate per unit area of cross section, then Leverett's experiments [36] were performed at $C_A = 0.1 - 1$, while the low rate floods [34] had $C_A \sim 10^{-4}$. In a reservoir $C_A = 10^{-4} - 10^{-6}$. As a consequence viscous forces were significant in determining the fluid configuration, and the resultant relative permeabilities are noticeably different from the values measured at lower rates. (Leverett [36] noted that at lower rates his measured relative permeabilities were lower, an observation consistent with our predictions.) We modeled the phase configurations in this experiment simply by filling available throats at random, with no selection due to effective radii. This simulates flow at a very high rate ($C_A \geq 1$), where capillary forces are no longer important. The predicted curves are again in good agreement with experiment, especially the nonwetting phase relative permeability.

Figure 6 shows low flow rate experimental curves obtained from a fired Berea sandstone with a porosity of

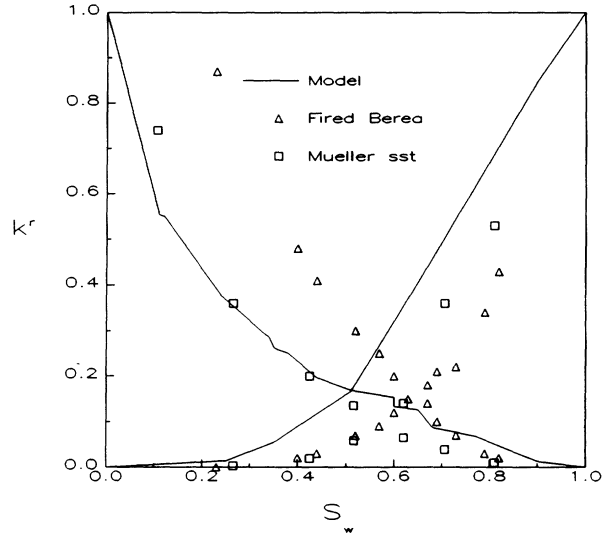


FIG. 6. Predicted and experimental measurements of capillary controlled drainage relative permeability in sandstone with a porosity of 23.9%. The triangles are measurements on fired Berea sandstone [2,4], which is only 80% quartz and consists of polydisperse sand grains. The squares are measurements on Mueller sandstone [37], which is 99.9% quartz and more monodisperse.

23.9% [2,4] and a Mueller sandstone with a porosity of 24% [37]. The model porous medium used to simulate these experiments were formed by swelling the spheres until a porosity of 24% was reached. The predicted capillary-controlled relative permeabilities are shown to match the Mueller experiment only. The Mueller sandstone is 99.9% quartz (grains plus cementing material) and is composed of grains of almost equal size; it thus conforms closely to the structure of our model porous media. The Berea sandstone, in contrast, is composed of grains of various sizes and is only 80% quartz. The remaining 20% is material that generally does not occur as solid concentric rims on the surfaces of the quartz grains. Thus the present network model is an inadequate representation of the pore structure of Berea sandstone. However, we expect that the simple model construction outlined here can be extended to account for more complicated rocks.

V. DISCUSSION

By carefully constructing a network model to represent the pore structure of a class of simple sandstones and by modeling two-phase flow through the network, we have been able to predict relative permeabilities in primary drainage, which compare well with experimental measurements on monominerallitic well-sorted materials. This comparison emphasizes the predictive power of our approach, in contrast to the essentially correlative nature of many previous calculations of relative permeability. The calculations depend only upon the accurately known microstructure of a real porous medium. Furthermore, the

predictions require no supplementary measurements on samples, such as capillary pressure as a function of saturation or estimates of pore throat size distributions from thin section images.

The model has already been validated against experimental measurements for single-phase flow for rocks composed of different materials and representing a wide range of porosities, so we know it is able to reproduce the major flow channels accurately. Also the invasion percolation model of drainage used to simulate two-phase flow is well established and has been shown to predict the fluid configuration in experimental network models [38]. The nonwetting phase resides in the centers of the pores and the larger throats and we are able to predict its relative permeability reliably. The configuration and flow of the wetting fluid is subtly controlled by the exact microstructure of the pore-grain surface, which we are unable to model precisely. Thus the predictions of the wetting phase relative permeability are less accurate.

It is not just the throat radius and pore volume distri-

butions that influence single- and two-phase flow—the pore-scale correlations in the geometry are also significant. The two biggest throats leading from a pore tend to be of the same size, while the smaller throats are randomly distributed. Using randomized throat radii and lengths in the calculation of absolute permeability on an unconsolidated sample overestimated the permeability by 78% [15]. A similar overestimate in the wetting phase relative permeability is also seen, although the nonwetting phase permeability is unaffected.

This work could be extended to investigate imbibition, the injection of a wetting fluid, and the behavior of more complex polydisperse sandstones. More significantly, however, this study is a step toward being able to quantify the sensitivity of relative permeability to rock structure and experimental conditions. For instance, we can now predict the change in relative permeability with compaction and cementation and correlate this change with porosity and absolute permeability, as well as indicate the effect of flow rate.

*Present address: BP Chemicals Ltd, P.O. Box 21, Bo'ness Road, Grangemouth, Stirlingshire FK3 9XH, United Kingdom.

- [1] I. Fatt, *Trans. AIME* **207**, 144 (1956).
- [2] S. J. Salter and K. K. Mohanty, in *Proceedings of the 57th Annual Technical Conference of the SPE-AIME*, New Orleans, Publication SPE 11017 (SPE, Richardson, TX, 1982).
- [3] A. A. Heiba, M. Sahimi, L. E. Scriven, and H. J. Davis, *SPE Reservoir Engineering* **7**, 123 (1992).
- [4] G. R. Jerauld and S. J. Salter, *Transp. Porous Media* **5**, 103 (1990).
- [5] R. Lenormand and C. Zarcone, *Transp. Porous Media* **4**, 599 (1989).
- [6] R. Lenormand, E. Touboul, and C. Zarcone, *J. Fluid Mech.* **189**, 165 (1988).
- [7] L. Furuberg, J. Feder, A. Aharony, and T. Jóssang, *Phys. Rev. Lett.* **61**, 2117 (1988).
- [8] C. E. Diaz, I. Chatzis, and F. A. L. Dullien, *Transp. Porous Media* **2**, 215 (1987).
- [9] M. M. Dias and A. C. Payatakes, *J. Fluid Mech.* **164**, 337 (1986).
- [10] A. J. Katz and A. H. Thompson, *Phys. Rev. B* **34**, 8179 (1986).
- [11] D. MacGowan, in *Proceedings of the European Conference of the Mathematics of Oil Production, Cambridge, 1989*, edited by P. R. King and S. F. Edwards (Oxford University Press, Cambridge, 1991).
- [12] J. Koplik, C. Lin, and M. Vermette, *J. Appl. Phys.* **56**, 3127 (1984).
- [13] M. Yanuka, F. Dullien, and D. Elrick, *J. Colloid Interface Sci.* **112**, 24 (1986).
- [14] J. Finney, Ph.D. dissertation, London University, 1968.
- [15] S. Bryant, P. R. King, and D. Mellor, *Transp. Porous Media* (to be published).
- [16] S. Bryant and C. Cade, in *Proceedings of the 3rd European Conference on the Mathematics of Oil Recovery*, edited by M. A. Christie *et al.* (Delft University Press, Delft, 1992).
- [17] M. J. Blunt, M. J. King, and H. Scher (unpublished).
- [18] B. Ripley, *Spatial Statistics* (Wiley, New York, 1981).
- [19] D. Mellor, Ph.D. dissertation, Open University, 1989.
- [20] G. Mason and D. Mellor, in *Characterization of Porous Solids II*, edited by F. Rodriguez-Reinoso *et al.* (Elsevier, Amsterdam, 1991).
- [21] J. Roberts and L. Schwartz, *Phys. Rev. B* **31**, 5990 (1985).
- [22] T. Bourbie and B. Zinszner, *J. Geophys. Res.* **90**, 11 524 (1985).
- [23] R. Chandler, J. Koplik, K. Lerman, and J. F. Willemsen, *J. Fluid Mech.* **119**, 249 (1982).
- [24] D. Wilkinson and J. F. Willemsen, *J. Phys. A* **16**, 3365 (1983).
- [25] M. Muskat and M. W. Meres, *Physics (N.Y.)* **7**, 346 (1936).
- [26] R. D. Wyckoff and H. G. Botset, *Physics (N.Y.)* **7**, 325 (1936).
- [27] P. G. de Gennes, *Physico-Chem. Hydrodyn.* **4**, 175 (1973).
- [28] S. Whitaker, *Transp. Porous Media* **1**, 105 (1986).
- [29] W. Rose, *Transp. Porous Media* **3**, 163 (1988).
- [30] J. C. Bacri, M. Chaouche, and D. Salin, *C. R. Acad. Sci. Paris* **311**, 591 (1990).
- [31] F. Kalaydjian, *Transp. Porous Media* **5**, 215 (1990).
- [32] D. Rothman, *J. Geophys. Res.* **95**, 8663 (1990).
- [33] M. C. Leverett, *Trans. AIME* **142**, 152 (1941).
- [34] J. Naar, R. Wygal, and J. Henderson, *Soc. Pet. Eng. J.* **131**, 13 (1962).
- [35] G. C. Topp and E. E. Miller, *Soil Sci. Soc. Am. Proc.* **30**, 156 (1966).
- [36] M. C. Leverett, *Trans. AIME* **132**, 149 (1939).
- [37] C. R. Sandberg, L. S. Gourlay, and R. F. Sippel, *Pet. Trans. AIME* **213**, 36 (1958).
- [38] R. Lenormand and C. Zarcone, *Phys. Rev. Lett.* **54**, 2226 (1985).